(μ-Oxo or hydroxo)bis(μ-carboxylato)diruthenium(III) complexes with tris(1-pyrazolyl)borate face-capping ligand, affording versatile oxidation states *via* a protonation/deprotonation couple

Tomoaki Tanase,*[a] Nao Takeshita,[a] Shigenobu Yano,*[a] Isamu Kinoshita[b] and Akio Ichimura[b]

[a] *Department of Chemistry, Faculty of Science, Nara Women's University, Kitauoya-higashi-machi, Nara 630, Japan*

[b] *Department of Chemistry, Faculty of Science, Osaka City University, Sumiyoshi-ku, Osaka 662, Japan*

NJC Letter

(μ-Oxo or μ-hydroxo)bis(μ-acetate)diruthenium(III) complexes with tris(1-pyrazolyl)borate, $[Ru_2^{III}(\mu\text{-}O)(\mu\text{-}CH_3COO)_2(HBpz_3)_2]$ (**1**) and $[Ru_2^{III}(\mu\text{-}OH)(\mu\text{-}CH_3COO)_2(HBpz_3)_2](PF_6)$ (**2**), have been prepared and characterized by X-ray crystallography, and showed a wide range of redox processes, $Ru_2^{II} \leftrightarrow Ru^{II}Ru^{III} \leftrightarrow Ru_2^{III} \leftrightarrow Ru^{III}Ru^{IV} \leftrightarrow Ru_2^{IV}$, coupled with protonation/deprotonation at the bridged monoatom.

Intensive studies have been focused on the non-heme diiron proteins, such as hemerythrin, R2 subunit of ribonucleotide reductase, and methane monooxygenase; these involve diiron active centers bridged by carboxylates and a mono-atom, oxo or hydroxo unit, and function by utilizing redox cycles coupled with dioxygen molecule.[1–3] A number of synthetic models with a (μ-oxo, hydroxo, or alkoxo)bis(μ-carboxylato) diiron(III) core have already been reported,[1–3] but, owing to their instability, those involving an Fe^{IV} center have not been studied in detail, in spite of their biorelevant importance. We have been interested in the parallel chemistry of (μ-oxo, hydroxo, or alkoxo)bis(μ-carboxylato)diruthenium complexes, hoping to obtain detailed structural and physical information of a wide variety of oxidation states from Ru_2^{II} to Ru_2^{IV} and to utilize their redox properties to mimic biological systems and to develop catalytic organic reactions.[4,5] The high valency oxo-bridged diruthenium complexes could also be useful artificial model systems for the oxygen evolving center of photosystem II.[6] We wish to report here the syntheses and structures of the (μ-oxo or hydroxo)bis(μ-carboxylato)-diruthenium(III) complexes with tris(1-pyrazolyl)borate face-capping ligand ($HBpz_3^-$), which affords a wide range of oxidation states *via* protonation and deprotonation of the mono-atom bridge. The neutral Ru_2^{III} complex, $[Ru_2^{III}(\mu\text{-}O)(\mu\text{-}CH_3COO)_2(HBpz_3)_2]$, has not been reported thus far, although its Fe_2^{III} counterpart, $[Fe_2^{III}(\mu\text{-}O)(\mu\text{-}CH_3COO)_2(HBpz_3)_2]$[7,8] has been reported as one of the seminal contributions on bioinorganic chemistry relevant to non-heme diiron proteins.

Reaction of $[Ru_2(CH_3COO)_4Cl]$[9] with two equiv. of sodium trispyrazolyl borate ($Na[HBpz_3]$) in methanol at room temperature afforded a neutral diruthenium(III) complex, $[Ru_2(\mu\text{-}O)(\mu\text{-}CH_3COO)_2(HBpz_3)_2]\cdot EtOH$ (**1**·EtOH) (27%).† Block-shaped crystals of $\mathbf{1}\cdot Et_2O$ were obtained from an ethanol–diethyl ether system. Treatment of **1**·EtOH with HPF_6 (60% in water) yielded violet rectangular crystals of $[Ru_2(\mu\text{-}OH)(\mu\text{-}CH_3COO)_2(HBpz_3)_2]\,(PF_6)\cdot Et_2O$ ($\mathbf{2}\cdot Et_2O$) in 58% yield.† The protonation and deprotonation proceeded reversibly in a quantitative manner based on the electronic spectral changes; characteristic absorption bands, λ/nm (log $\varepsilon/M^{-1}\,cm^{-1}$), were observed at 570 (4.143) and 276 (4.288) for **1** and 544 (3.898), 394 (3.623), 338 (3.699) and 252 (4.215) for **2**. Complex **1** was diamagnetic on the basis of the ^1H NMR spectrum, whereas the ^1H NMR spectrum of **2** showed isotropically shifted features for δ from −6 to 8 ppm owing to its paramagnetism.

† *Experimental and analytical data for* **1**·EtOH. The blue major band on the alumina column (10% deactivated) eluted with dichloromethane was collected and concentrated to dryness. The residue was crystallized from hot ethanol to give microcrystals of **1**·EtOH in 27% yield. Anal. calcd for $C_{24}H_{32}N_{12}O_6Ru_2B_2$ (F_w 808.56): C, 35.65; H, 3.99; N, 20.79. Found: C, 35.31; H, 4.04; N, 21.05%.

For $\mathbf{2}\cdot Et_2O$. Complex **1**·EtOH was treated with HPF_6 (1 equiv. 60% water solution) in a CH_2Cl_2–CH_3OH mixed solvent at room temperature. The mixture was concentrated to dryness and the residue was crystallized from a CH_2Cl_2–Et_2O mixed solvent to afford violet crystals of $\mathbf{2}\cdot Et_2O$ in 58% yield. Anal. calcd for $C_{26}H_{37}N_{12}O_6Ru_2B_2PF_6$ (F_w 982.58): C, 31.78; H, 3.80; N, 17.11. Found: C, 32.16; H, 3.91; N, 17.40%.

For $\mathbf{3}\cdot 0.5CH_2Cl_2$. Complex **1**·EtOH was treated with $(NH_4)_2$-$Ce(NO_3)_6$ and NH_4PF_6 in acetonitrile for 1–2 h at room temperature. The solvent was removed under reduced pressure and the residue was extracted with CH_2Cl_2 and crystallized from a CH_2Cl_2–Et_2O solvent system to give violet crystals of $\mathbf{3}\cdot 0.5CH_2Cl_2$ in 72% yield. Anal. calcd for $C_{22.5}H_{27}N_{12}O_5Ru_2B_2ClPF_6$ (F_w 949.92): C, 28.46; H, 2.87; N, 17.70. Found: C, 28.75; H, 2.98; N, 17.48%.

The structures of **1** and **2** were shown by X-ray crystallography to involve biorelevant (μ-oxo)bis(μ-acetate)- and (μ-hydroxo)bis(μ-acetate)-diruthenium(III) cores, respectively (Fig. 1 and 2).‡ The complex **1** consists of two Ru^{III} octahedra bridged by an oxo and two acetate ligands with two face-capping $HBpz_3^-$ ligands (Fig. 1). The (μ-oxo)bis(μ-acetate)diruthenium(III) core is essentially identical to those of cationic compounds $[Ru_2(\mu\text{-}O)(\mu\text{-}CH_3COO)_2(Me_3tacn)_2]^{2+}$ (Me_3tacn = 1,4,7 - trimethyl - 1,4,7 - triazacyclononane),[10,11]

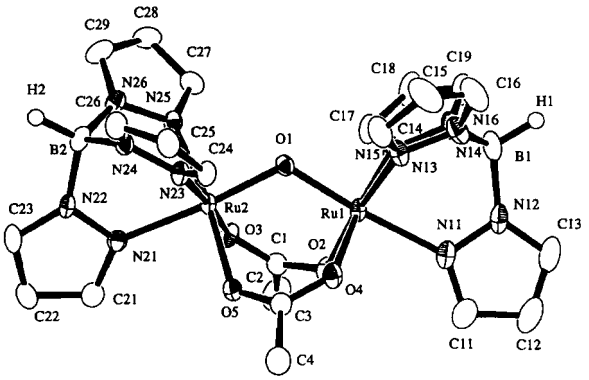

Fig. 1 ORTEP diagram of the complex **1** showing 40% probability ellipsoids. Selected distances/Å and angles/°: Ru(1)···Ru(2) = 3.2544(7), Ru(1)—O(1) = 1.868(3), Ru(1)—O(2) = 2.085(3), Ru(1)—O(4) = 2.080(3), Ru(1)—N(11) = 2.130(4), Ru(1)—N(13) = 2.040(4), Ru(1)—N(15) = 2.038(4), Ru(2)—O(1) = 1.858(3), Ru(2)—O(3) = 2.072(3), Ru(2)—O(5) = 2.090(3), Ru(2)—N(21) = 2.118(4), Ru(2)—N(23) = 2.039(4), Ru(2)—N(25) = 2.042(4), O(1)—Ru(1)—O(2) = 97.3(1), O(1)—Ru(1)—O(4) = 91.9(1), O(1)—Ru(1)—N(11) = 175.5(1), O(1)—Ru(1)—N(13) = 88.4(1), O(1)—Ru(1)—N(15) = 94.0(1), O(2)—Ru(1)—O(4) = 89.3(1), O(2)—Ru(1)—N(13) = 173.9(1), O(4)—Ru(1)—N(15) = 174.1(1), N(11)—Ru(1)—N(13) = 87.1(2), N(11)—Ru(1)—N(15) = 85.4(1), N(13)—Ru(1)—N(15) = 87.5(2), O(1)—Ru(2)—O(3) = 92.0(1), O(1)—Ru(2)—O(5) = 96.8(1), O(1)—Ru(2)—N(21) = 176.3(1), O(3)—Ru(2)—O(5) = 89.9(1), O(3)—Ru(2)—N(23) = 175.4(1), O(5)—Ru(2)—N(25) = 173.1(1), N(21)—Ru(2)—N(23) = 86.4(1), N(21)—Ru(2)—N(25) = 86.7(1), N(23)—Ru(2)—N(25) = 87.0(1), Ru(1)—O(1)—Ru(2) = 121.7(2)

‡ *Crystal data* **1** · Et_2O. ($C_{26}H_{36}N_{12}O_6B_2Ru_2$, F_w = 836.41), T = −117 °C, monoclinic space group $P2_1/c$, a = 14.457(3), b = 13.068(3), c = 18.727(2) Å, β = 104.00(1)°, V = 3433.0(9) Å^3, Z = 4. A blue block-shaped crystal 0.45 mm × 0.30 mm × 0.10 mm was fixed on the top of a glass fiber with Paraton N oil. 8195 reflections ($4° < 2\theta < 55°$) were measured on a Rigaku AFC7R diffractometer with graphite monochromated Mo-Kα radiation. An absorption correction by ψ-scan method was applied (μ = 9.38 cm^{-1}). The structure was solved by direct methods using the program SIR92 and was refined to R = 0.039 and R_w = 0.047 for 5771 independent reflections with $I > 3\sigma(I)$. All non-hydrogen atoms were refined anisotropically and the hydrogen atoms were located from difference Fourier syntheses and were refined isotropically.

Crystal data **2**·Et_2O. ($C_{26}H_{37}N_{12}O_6B_2PF_6Ru_2$, F_w = 982.38), T = −118 °C, monoclinic space group $P2_1/n$, a = 11.989(4), b = 19.849(6), c = 16.361(5) Å, β = 104.11(2)°, V = 3775(1) Å^3, Z = 4. A violet rectangular crystal 0.47 mm × 0.23 mm × 0.10 mm was fixed on the top of a glass fiber with Paraton N oil, and 6824 reflections ($4° < 2\theta < 50°$) were measured on a Rigaku AFC7R diffractometer with graphite monochromated Mo-Kα radiation. An absorption correction by ψ-scan method was applied (μ = 9.29 cm^{-1}) The structure was solved by direct methods using the program SIR92 and was refined to R = 0.035 and R_w = 0.042 for 5072 independent reflections with $I > 3\sigma(I)$. All non-hydrogen atoms were refined anisotropically and the hydrogen atoms were located from difference Fourier syntheses and were refined isotropically. All calculations were carried out on a Silicon Graphics Indigo Station with teXsan program system.

Supplementary data available from the Cambridge Crystallographic Data Centre, reference 440/046.

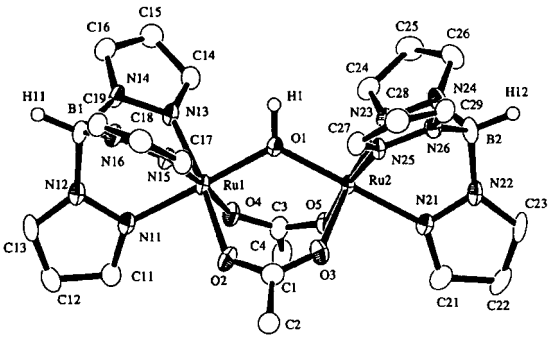

Fig. 2 ORTEP diagram of the complex cation of **2** showing 40% probability ellipsoids. Selected distances/Å and angles/°: Ru(1)···Ru(2) = 3.4490(9), Ru(1)—O(1) = 1.957(3), Ru(1)—O(2) = 2.080(4), Ru(1)—O(4) = 2.065(3), Ru(1)—N(11) = 2.034(4), Ru(1)—N(13) = 2.030(4), Ru(1)—N(15) = 2.031(4), Ru(2)—O(1) = 1.960(3), Ru(2)—O(3) = 2.069(4), Ru(2)—O(5) = 2.074(3), Ru(2)—N(21) = 2.033(4), Ru(2)—N(23) = 2.040(4), Ru(2)—N(25) = 2.022(4), O(1)—H(1) = 1.03(5), O(1)—Ru(1)—O(2) = 92.6(1), O(1)—Ru(1)—O(4) = 91.5(1), O(1)— Ru(1)—N(11) = 179.1(1), O(1)—Ru(1)—N(13) = 91.8(1), O(1)—Ru(1)—N(15) = 94.4(1), O(2)—Ru(1)—O(4) = 92.1(1), O(2)—Ru(1)—N(13) = 174.8(1), O(4)—Ru(1)—N(15) = 174.1(1), N(11)—Ru(1)—N(13) = 87.3(2), N(11)—Ru(1)—N(15) = 85.8(1), N(13)—Ru(1)—N(15) = 88.6(1), O(1)—Ru(2)—O(3) = 90.9(1), O(1)—Ru(2)—O(5) = 92.4(1), O(1)—Ru(2)—N(21) = 179.2(1), O(3)—Ru(2)—O(5) = 93.1(1), O(3)—Ru(2)—N(23) = 173.7(1), O(5)—Ru(2)—N(25) = 174.6(1), N(21)—Ru(2)—N(23) = 86.6(2), N(21)—Ru(2)—N(25) = 86.8(1), N(23)—Ru(2)—N(25) = 88.3(1), Ru(1)—O(1)—Ru(2) = 123.4(2). Ru(1)—O(1)—H(1) = 118(2), Ru(2)—O(1)—H(1) = 118(2)

$[Ru_2(\mu\text{-}O)(\mu\text{-}CH_3COO)_2(py)_6]^{2+}$ (py = pyridine),[12] $[Ru_2(\mu\text{-}O)(\mu\text{-}CH_3COO)_2(1\text{-}MeIm)_6]^{2+}$ (1-MeIm = 1-methyl imidazol),[13] and $[Ru_2(\mu\text{-}O)(\mu\text{-}O_2P(O)(OH))_2(tpm)_6]$ [tpm = tris(1-pyrazolyl)methane].[14] The complex cation of **2** involves a (μ-OH)(μ-$CH_3COO)_2Ru_2^{III}$ core with two $HBpz_3^-$ ligands capping the facial sites. The hydrogen atom, H(1), of the OH group is unambiguously determined by difference Fourier synthesis. The bridging oxygen atom, O(1), has an essentially sp^2 character, the sum of bond angles being 359°, and the (μ-OH) Ru_2 unit takes a planar arrangement. The Ru···Ru distance in **2** [3.4490(9) Å] is dramatically elongated in comparison with that in **1** [3.2544(7) Å], mainly ascribable to the $Ru—O_{hydroxo}$ bond lengths (average 1.955 Å) being longer than the $Ru—O_{oxo}$ ones (average 1.855 Å). This is the first structurally characterized example of the (μ-hydroxo)bis(μ-carboxylato)diruthenium(III) complex, Wieghardt and co-workers having briefly reported the preliminary data for the crystal structure of $[Ru_2^{III}(\mu\text{-}OH)(\mu\text{-}CH_3COO)_2(tacn)_2]^{3+}$ [Ru···Ru = 3.472(2) Å].[11] Recently, Yamaguchi and co-workers[15] have reported the Ru···Ru distances for $[Ru_2^{III}(\mu\text{-}OH)(\mu\text{-}CH_3COO)_2(bpy)_2L_2]^{3+}$ [L = py (**4**), 1-methylimidazole (**5**)] determined by EXAFS analyses as 3.54 (**4**) and 3.48 Å (**5**), which are rather longer than the present value. It should be noted that the structural geometry of **2** is closely similar to its iron counterpart, $[Fe_2^{III}(\mu\text{-}OH)(\mu\text{-}CH_3COO)_2(HBpz_3)_2]^+$ [Fe···Fe = 3.439(1) Å, $Fe—O_{oxo}$ = 1.956 Å, Fe—O—Fe = 123.1(2)°].[16]

The electrochemical properties of complexes **1** and **2** were analyzed by cyclic voltammetry (Fig. 3). The cyclic voltammogram (CV) of **1** in acetonitrile containing 0.1 M $[Bu^n_4N][PF_6]$ as supporting electrolyte [Fig. 3(*a*)] showed two reversible oxidation waves at 0.17 V ($E^{ox1}_{1/2}$) *vs.* Ag/$AgPF_6$ and 1.35 V ($E^{ox2}_{1/2}$), which could correspond to $[Ru_2^{III}(\mu\text{-}O)(\mu\text{-}CH_3COO)_2L_2]/[Ru^{III}Ru^{IV}(\mu\text{-}O)(\mu\text{-}CH_3COO)_2L_2]^+$ and $[Ru^{III}Ru^{IV}(\mu\text{-}O)(\mu\text{-}CH_3COO)_2L_2]^+/Ru_2^{IV}(\mu\text{-}O)(\mu\text{-}CH_3COO)_2L_2]^{2+}$ (L = $HBpz_3^-$) redox processes on the basis of coulometric analyses. The extremely large half-potential separation, $\Delta E^{ox} = |E^{ox1}_{1/2} - E^{ox2}_{1/2}| = 1.18$ V, implied that the mixed-valent $Ru^{III}Ru^{IV}(\mu\text{-}O)$ complex is remarkably stable, with the conproportionation constant K_c^5 for

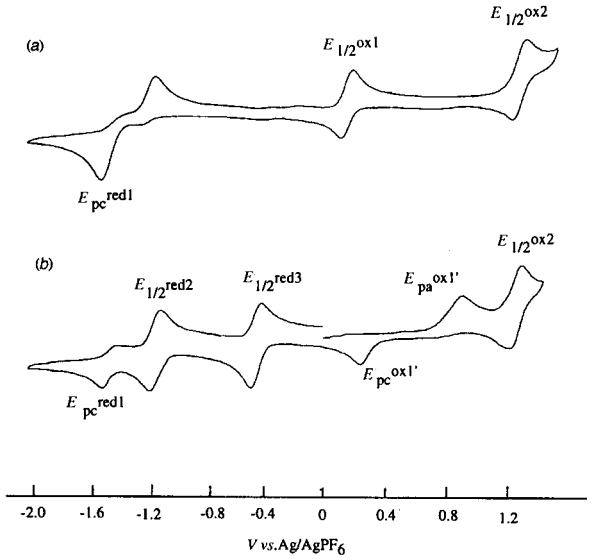

Fig. 3 Cyclic voltammograms of **1** (*a*) and **2** (*b*) in acetonitrile (0.1 M) $[Bu_4^nN][PF_6]$ with a glassy carbon working electrode and an $Ag/AgPF_6$ reference electrode at a scan rate of 100 mV s^{-1} at room temperature. The wave at E_{pc}^{red1} of **2** (*b*) disappeared upon addition of *p*-toluene sulfonic acid

$Ru_2^{III} + Ru_2^{IV} \rightleftharpoons 2Ru^{III}Ru^{IV}$ being 9.1×10^{19}. In fact, a potentiostatic electrolysis of **1** at 0.7 V consumed 1 F per dimer to afford $[Ru^{III}Ru^{IV}(\mu\text{-}CH_3COO)_2L_2](PF_6)$ (**3**), which was also prepared by the oxidation of **1** with $(NH_4)_2Ce(NO_3)_6$ in the presence of NH_4PF_6.† The CV of **1** exhibited only one irreversible reduction wave at −1.52 V (E_{pc}^{red1}), suggesting two-electron reduction of **1** to Ru_2^{II} species followed by a structural change of the dinuclear core. The CV of **2** [Fig. 3(*b*)], protonated at the oxo bridge, dramatically changed and showed two reversible reduction processes at −1.14 V ($E_{1/2}^{red2}$) and −0.45 V ($E_{1/2}^{red3}$). The coulometric analyses indicated that they were assignable to two-step one-electron transfer series of $[Ru_2^{II}(\mu\text{-}OH)(\mu\text{-}CH_3COO)_2L_2]^- \rightleftharpoons [Ru^{II}Ru^{III}(\mu\text{-}OH)(\mu\text{-}CH_3COO)_2L_2] \rightleftharpoons [Ru_2^{III}(\mu\text{-}OH)(\mu\text{-}CH_3COO)_2L_2]^+$. The $Ru^{II}Ru^{III}$ mixed-valence species is estimated to be fairly stable from the large half-potential separation, $\Delta E^{red} = |E_{1/2}^{red2} - E_{1/2}^{red3}| = 690$ mV ($K_c = 4.7 \times 10^{11}$). The CV in the positive potential showed a redox couple at 0.95 V ($E_{pa}^{ox1'}$) and 0.25 V ($E_{pc}^{ox1'}$), which is assumed to involve an electrochemical process as indicated in Scheme 1, and also showed the $[Ru^{III}Ru^{IV}(\mu\text{-}O)(\mu\text{-}CH_3COO)_2L_2]^+/[Ru_2^{IV}(\mu\text{-}O)(\mu\text{-}CH_3COO)_2L_2]^{2+}$ process at $E_{1/2}^{ox2}$. The electrochemical study clearly demonstrated that a wide range of oxidation states, from Ru_2^{II} to Ru_2^{IV}, could be accessible from the diruthenium(III) complexes **1** and **2** and that the protonation/deprotonation at the monoatom bridge dramatically switched the redox processes.

We are now trying to isolate the high and low valency diruthenium species (Ru_2^{IV} and Ru_2^{II}), the reactivity and physical properties of which could be very useful for mimicking biological metabolisms of small molecules.

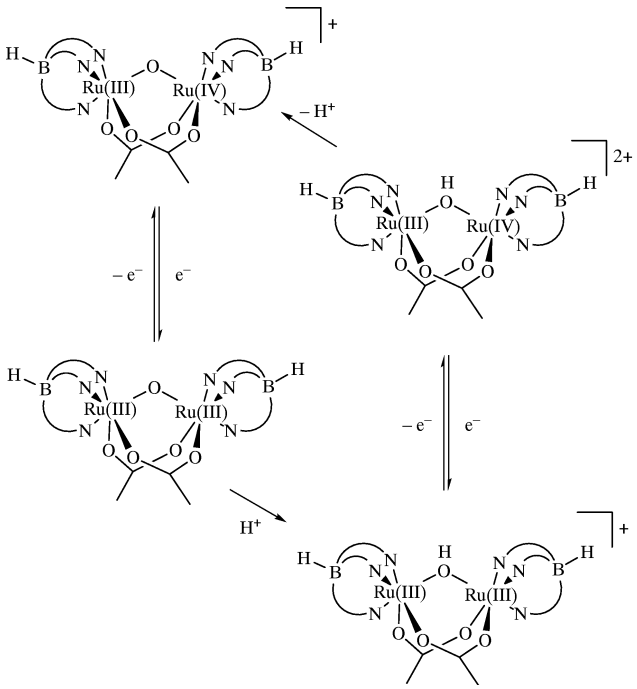

Scheme 1 Proton-coupled redox processes at $E_{pc}^{ox1'}$ and $E_{pa}^{ox1'}$

Acknowledgements

The authors thank Professor Yoichi Sasaki of Hokkaido University for helpful discussion. This work was partially supported by a Grant-in-Aid for Scientific Research from the Ministry of Education of Japan (no. 10131247etc), and Grants from Iwatani, Nippon Itagarasu, Mitsubishi-Yuka, and Nagase Foundations and the San-Ei Gen Foundation for Food Chemical Research.

References

1 S. J. Lippard, *Angew. Chem., Int. Ed. Engl.*, 1988, **27**, 344.
2 D. M. J. Kurtz, *Chem. Rev.*, 1990, **90**, 585.
3 A. L. Feig and S. J. Lippard, *Chem. Rev.*, 1994, **94**, 759.
4 T. Tanase, M. Kato, Y. Yamada, K. Tanaka, K. Lee, Y. Sugihara, T. Nagano and S. Yano, *Chem. Lett.*, 1994, 1853.
5 T. Tanase, Y. Yamada, K. Tanaka, T. Miyazu, M. Kato, K. Lee, Y. Sugihara, W. Mori, A. Ichimura, I. Kinoshita, Y. Yamamoto, M. Haga, Y. Sasaki and S. Yano, *Inorg. Chem.*, 1996, **35**, 6230.
6 W. Ruttinger and G. C. Dismukes, *Chem. Rev.*, 1997, **97**, 1.
7 W. H. Armstrong and S. J. Lippard, *J. Am. Chem. Soc.*, 1983, **105**, 4837.
8 W. H. Armstrong, A. Spool, G. C. Papaefthymiou, R. B. Frankel and S. J. Lippard, *J. Am. Chem. Soc.*, 1984, **106**, 3653.
9 R. W. Mitchell, A. Spencer and G. Wilkinson, *J. Chem. Soc., Dalton Trans.*, 1973, 846.
10 P. Neubold, K. Wieghardt, B. Nuber and J. Weiss, *Angew. Chem., Ind. Ed. Engl.*, 1988, **27**, 933.
11 P. Neubold, K. Wieghardt, B. Nuber and J. Weiss, *Inorg. Chem.*, 1989, **28**, 459.
12 Y. Sasaki, M. Suzuki, A. Nagasawa, A. Tokiwa, M. Ebihara, T. Yamaguchi, C. Kabuto, T. Ochi and T. Ito, *Inorg. Chem.*, 1991, **30**, 4903.
13 C. Sudha, S. K. Mandal and A. R. Chakravarty, *Inorg. Chem.*, 1993, **32**, 3801.
14 A. Llobet, M. E. Curry, H. T. Evans and T. J. Meyer, *Inorg. Chem.*, 1989, **28**, 3131.
15 M. Valli, S. Miyata, H. Wakita, T. Yamaguchi, A. Kikuchi, K. Umakoshi, T. Imamura and Y. Sasaki, *Inorg. Chem.*, 1997, **36**, 4622.
16 W. H. Armstrong and S. J. Lippard, *J. Am. Chem. Soc.*, 1984, **106**, 4632.

Received in Cambridge, UK, 15*th April* 1998;
Letter 8/04617D